Developmental stages of tertiary lymphoid tissue reflect local injury and inflammation in mouse and human kidneys

OPEN

Yuki Sato[1,2], Peter Boor[3,4], Shingo Fukuma[5], Barbara M. Klinkhammer[3,4], Hironori Haga[6], Osamu Ogawa[7], Jürgen Floege[4] and Motoko Yanagita[1,8]

[1]Department of Nephrology, Graduate School of Medicine, Kyoto University, Kyoto, Japan; [2]Medical Innovation Center TMK Project, Graduate School of Medicine, Kyoto University, Kyoto, Japan; [3]Institute of Pathology, Rhenish-Westphalian Technical University of Aachen, Aachen, Germany; [4]Department of Nephrology, Rhenish-Westphalian Technical University of Aachen, Aachen, Germany; [5]Human Health Sciences, Graduate School of Medicine, Kyoto University, Kyoto, Japan; [6]Department of Diagnostic Pathology, Kyoto University Hospital, Kyoto, Japan; [7]Department of Urology, Graduate School of Medicine, Kyoto University, Kyoto, Japan; and [8]Institute for the Advanced Study of Human Biology (ASHBi), Kyoto University, Kyoto, Japan

Tertiary lymphoid tissues (TLTs) are inducible ectopic lymphoid tissues in chronic inflammatory states and function as sites of priming local immune responses. We previously demonstrated that aged but not young mice exhibited multiple TLTs after acute kidney injury and that TLTs were also detected in human aged and diseased kidneys. However, the forms of progression and the implication for kidney injury remain unclear. To clarify this we analyzed surgically resected kidneys from aged patients with or without chronic kidney disease as well as kidneys resected for pyelonephritis, and classified TLTs into three distinct developmental stages based on the presence of follicular dendritic cells and germinal centers. In injury-induced murine TLT models, the stages advanced with the extent of kidney injury, and decreased with dexamethasone accompanied with improvement of renal function, fibrosis and inflammation. Kidneys from aged patients with chronic kidney disease consistently exhibited more frequent and advanced stages of TLTs than those without chronic kidney disease. Kidneys of patients with pyelonephritis exhibited more frequent TLTs with more advanced stages than aged kidneys. Additionally, TLTs in both cohorts shared similar locations and components, suggesting that TLT formation may not be a disease-specific phenomenon but rather a common pathological process. Thus, our findings provide the insights into biological features of TLT in the kidney and implicate TLT stage as a potential marker reflecting local injury and inflammation.

Kidney International (2020) ■, ■–■; https://doi.org/10.1016/j.kint.2020.02.023

KEYWORDS: follicular dendritic cell; renal aging; renal inflammation; tertiary lymphoid tissues

Correspondence: *Motoko Yanagita, Department of Nephrology, Graduate School of Medicine, Kyoto University, Shogoin-Kawahara-cho 54, Sakyo-ku, Kyoto 606-8507, Japan. E-mail: motoy@kuhp.kyoto-u.ac.jp*

Received 1 October 2018; revised 18 February 2020; accepted 20 February 2020

Tertiary lymphoid tissues (TLTs) are ectopic lymphoid tissues that are formed under various pathologic conditions such as autoimmunity and infection.[1–3] TLTs are composed of a hematopoietic compartment, which comprises mostly T and B cells, and stromal components, in particular fibroblasts. The basic functions of TLTs are similar to those of secondary lymphoid organs such as lymph nodes.[1–3] TLTs have the potential to initiate adaptive immune responses and produce large amounts of proinflammatory cytokines. Additionally, some TLTs develop germinal centers, unique structures in which B cells proliferate rapidly and undergo class switching, resulting in the generation of antibody-secreting plasma cells. Besides these functional similarities, TLTs and secondary lymphoid organs also rely on related molecules for their development, including the homeostatic CXC chemokine ligand 13 (CXCL13) and retinoic acid.[1–5]

The role of TLT in the host organ is context-dependent and can be beneficial or detrimental.[1–3] In patients with rheumatoid arthritis, for instance, multiple TLTs develop in the synovium and generate pathogenic autoantibodies such as anti-cyclic citrullinated protein → peptide antibodies, which are used as a specific, diagnostic, and prognostic marker of rheumatoid arthritis.[6–9] In contrast, during infections, TLTs are induced as an integral part of anti-pathogen immunity at local site, though a failure to eradicate a pathogen can lead to the development of autoimmunity. In a previous study, we found that aged but not young mice developed multiple renal TLTs after acute kidney injury.[10] TLTs occupied a broad area of renal parenchyma and promoted inflammation. The TLT size was closely associated with impaired renal function and increased expression of proinflammatory cytokines such as tumor necrosis factor-α and interferon-γ.[10] Additionally, depletion of CD4-positive cells as well as dexamethasone treatment prevented TLT formation and improved renal

Table 1 | Clinical characteristics of German patients with pyelonephritis evaluated in the study

Patients	Total
Pyelonephritis (*n*)	16
Age (yr)	
Average	52.9
Median	52.0
Range	22.0–86.0
Male (female) (%)	25 (75)
Serum Cr (mg/dl)	
Average	1.17
Median	1.12
Range	0.70–3.20

Cr, creatinine.
A diagnosis of pyelonephritis was based both on clinical and histologic findings compatible with pyelonephritis.

outcomes.[10] Although these interventions did not specifically target TLTs, we speculated that age-dependent formation of TLTs in the diseased kidneys was detrimental for the host.[10,11]

TLTs were also detected in aged human kidneys, with a composition similar to those of mouse TLTs.[10] In addition to aged human kidneys, TLTs were observed in kidneys of patients with autoimmune diseases,[12] renal allograft rejection,[13,14] and in IgA nephropathy.[15] However, the comprehensive understanding of TLTs in human kidney is still lacking,[16] and little information is available on their precise incidence, causes, variation in different etiologies, and clinical relevance. One of the reasons for this may be that most of the prior investigations of renal TLT relied on a small number of patients or TLTs from limited kidney tissue obtained via needle biopsy, which might not be sufficient to representatively reflect renal TLTs. In addition, though renal biopsy remains an important tool in the management of kidney diseases and provides prognostic information independent of clinical predictors such as proteinuria,[17] the indication of renal biopsy is limited to certain chronic kidney disease (CKD) populations because of the risk for complications such as bleeding. Another reason is that the phenotypic heterogeneity of TLTs complicated our understanding of the clinical relevance of TLTs in human kidneys. TLTs develop postnatally through a multistep process that might contribute to their heterogeneity.[1–3] The accurate and reliable recognition of TLTs and their developmental stages seems a prerequisite for better understanding of TLTs in human kidneys. To date, however, the extent of TLT heterogeneity has not been explored, especially in human kidneys, and the relationship between the heterogeneity and disease severity also remains unclear.

In this study, we analyzed surgically resected human kidney samples from patients with pyelonephritis, because infection is a strong trigger of TLT development in various tissues[1–3] and found multiple TLTs developed in human pyelonephritis kidneys. Combined with the data from aged patients and the aged murine model we have established,[10] we provide evidence that TLT formation is a common pathogenic process that proceeds through several distinct developmental stages irrespective of etiology. Furthermore, we established a phenotypic evaluation method for TLTs in human kidneys based on the presumed developmental stages and showed that the TLT stages were associated with the severity of kidney injury in mice and humans and could be reversible even after TLTs mature into advanced stages.

RESULTS

Human pyelonephritis kidneys show multiple lymphocyte aggregates

Infection is a strong trigger of TLT development in various tissues,[1–3] but whether TLTs form in human pyelonephritic kidneys has not been investigated. To investigate this, we examined sections of kidneys surgically removed because of pyelonephritis. The clinical features of these patients are listed in Table 1. We confirmed that kidneys of the patients with pyelonephritis exhibited diffuse interstitial scarring and tubular atrophy with thyroidization and in some cases acute pyelonephritis with infiltrates of neutrophils (Supplementary Figure S1A–C), all of which are typical histologic findings in pyelonephritic kidneys.[18,19] Pyelonephritic kidneys exhibited multiple mononuclear cell aggregates with a unique distribution (Figure 1). A chain of aggregates appeared just under the renal capsule and near the corticomedullary junction (Figure 1a; Supplementary Figure S2A), preferentially in close proximity to blood and lymphatic vessels (Figure 1c; Supplementary Figure S3). Additionally, aggregates were found along glomeruli (Figure 1d), developing in the perirenal tissue, hilus, and submucosa of the renal pelvis (Supplementary Figure S2B–D). This localization of aggregates in pyelonephritic kidneys was similar to that of aged kidneys (Supplementary Figure S4). Almost no aggregates were detectable in mildly injured areas (Supplementary Figure S5A). In contrast, in more severely injured regions, larger aggregates were noted (Supplementary Figure S5B and C). There were no inflammatory cellular aggregates in the medulla, although tissue destruction was detected broadly (Supplementary Figure S5D). These aggregates were composed mainly of T and B lymphocytes (Figure 1b, e, and f).

Cellular and molecular components of TLTs in pyelonephritis are similar to those of age-dependent TLTs

In the present study, we defined TLTs as the organized lymphocyte aggregates with signs of proliferation. Immunohistochemical analysis revealed major intra- and interpatient heterogeneity in TLT phenotypes (the list of markers related with TLTs in human kidneys is presented in Supplementary Table S1). TLTs with no distinct T- and B-cell area (Figure 2a and b) but with α-smooth muscle actin (α-SMA)–positive fibroblastic network (Figure 2c) were observed in regions with relatively mild injury. In contrast, TLTs in highly destroyed areas harbored organized B-cell follicles, surrounded by T cells (Figure 2d). CD21-positive follicular dendritic cell (FDC), a dendritic-shape stromal cell in charge of organizing B-cell homeostasis and humoral immune responses in secondary lymphoid organs,[20] formed B-cell

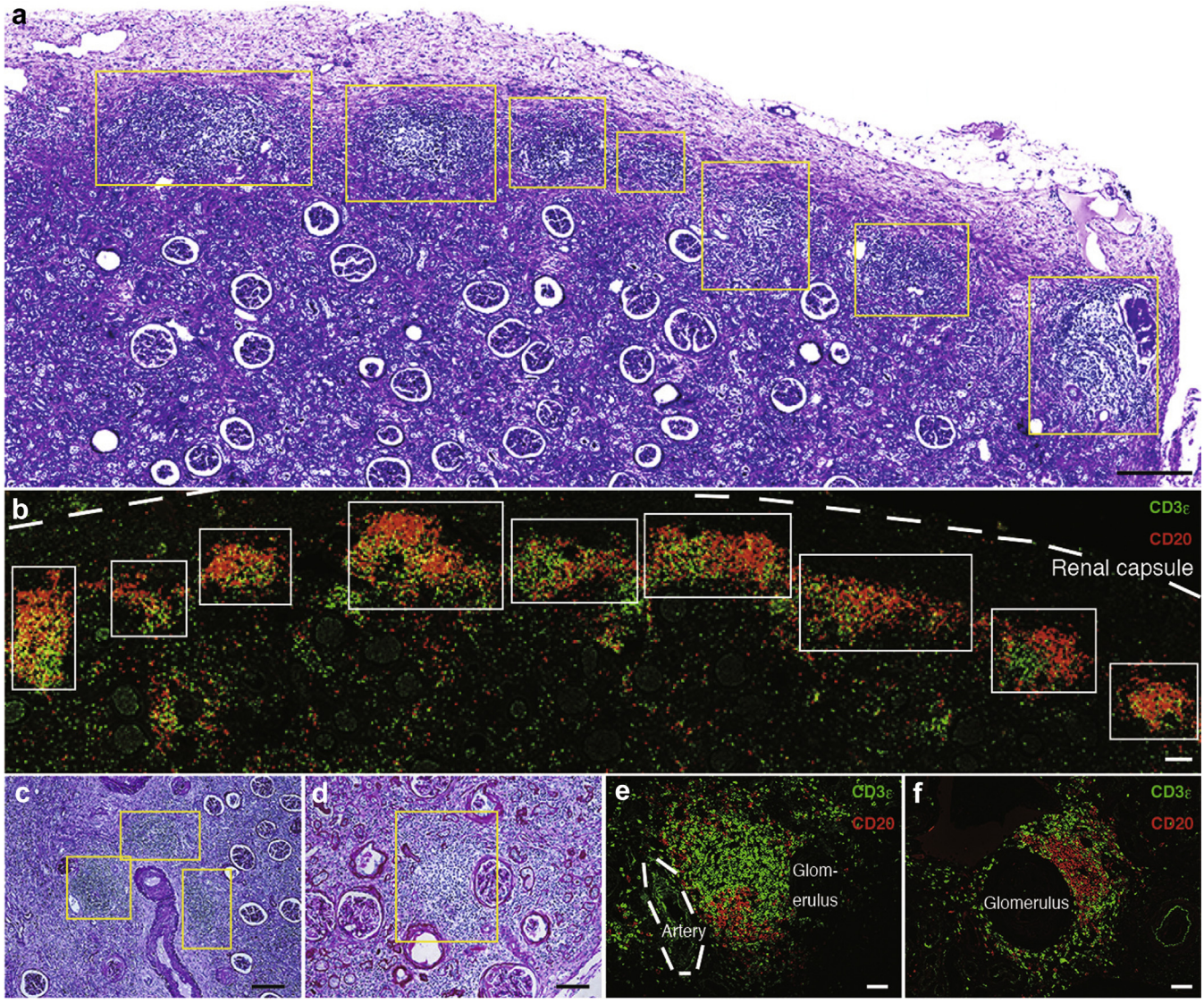

Figure 1 | Human pyelonephritic kidneys exhibited multiple lymphocyte aggregates. Histological analysis of human pyelonephritic kidneys. (**a,c,d**) Periodic acid–Schiff staining showed a chain of aggregates extending over long areas (**a**) just under the renal capsule and (**c**) multiple aggregates around blood vessels and (**d**) in periglomerular areas. (**b,e,f**) Immunofluorescence of CD3ε (a T-cell marker) and CD20 (a B-cell marker) in areas (**b**) just under the renal capsule, (**e**) around blood vessels, and (**f**) in glomeruli. Yellow and white boxes indicate the localization of aggregates. The white dotted line in part (**b**) indicates the renal capsule, whereas the dotted line in part (**e**) indicates the location of an artery. Bars = (**a**) 300 μm, (**b,d**) 100 μm, (**c**) 200 μm, and (**e,f**) 50 μm. To optimize viewing of this image, please see the online version of this article at www.kidney-international.org.

follicles (Figure 2d and e). Additionally, some of the aggregates with an FDC network developed B-lymphocyte clusters with pronounced proliferative activity (Figure 2f), indicating the formation of germinal centers. Plasma cells were also detectable around TLTs (Figure 2g), suggesting the occurrence of B-cell maturation in TLTs. Homeostatic chemokine CXCL13-positive cells including FDCs were detected within aggregates, and they were negative for CD45 (Figure 2h and i). FDCs were positive for p75 neurotrophin receptor, a neural crest marker (Figure 2k), and were surrounded by fibroblast-like cells positive for retinaldehyde dehydrogenases 2, a rate-limiting enzyme in retinoic acid synthesis (Figure 2j), as we previously reported in aged human kidneys.[10] T cells within TLTs were mainly CD4-positive (Figure 2l and m), some of which were positive for Foxp3[21,22], a master regulator of regulatory T cells[21] (Supplemental Figure S6). Macrophages were detectable around TLTs, but they were sparse inside TLTs (Figure 2n and o). These cellular and molecular components of TLTs in pyelonephritic kidneys showed marked similarity to those in age-dependent TLTs.[10] We also found that some of the CD21-positive FDC networks were composed of 2 subdomains (Supplementary Figure S7A and B): the proliferating B-cell cluster area with CD21 weakly positive FDC area and the scattered proliferating B-cell area with CD21 strongly positive FDC area. This is reminiscent of the dark zone and light zone of germinal center in secondary

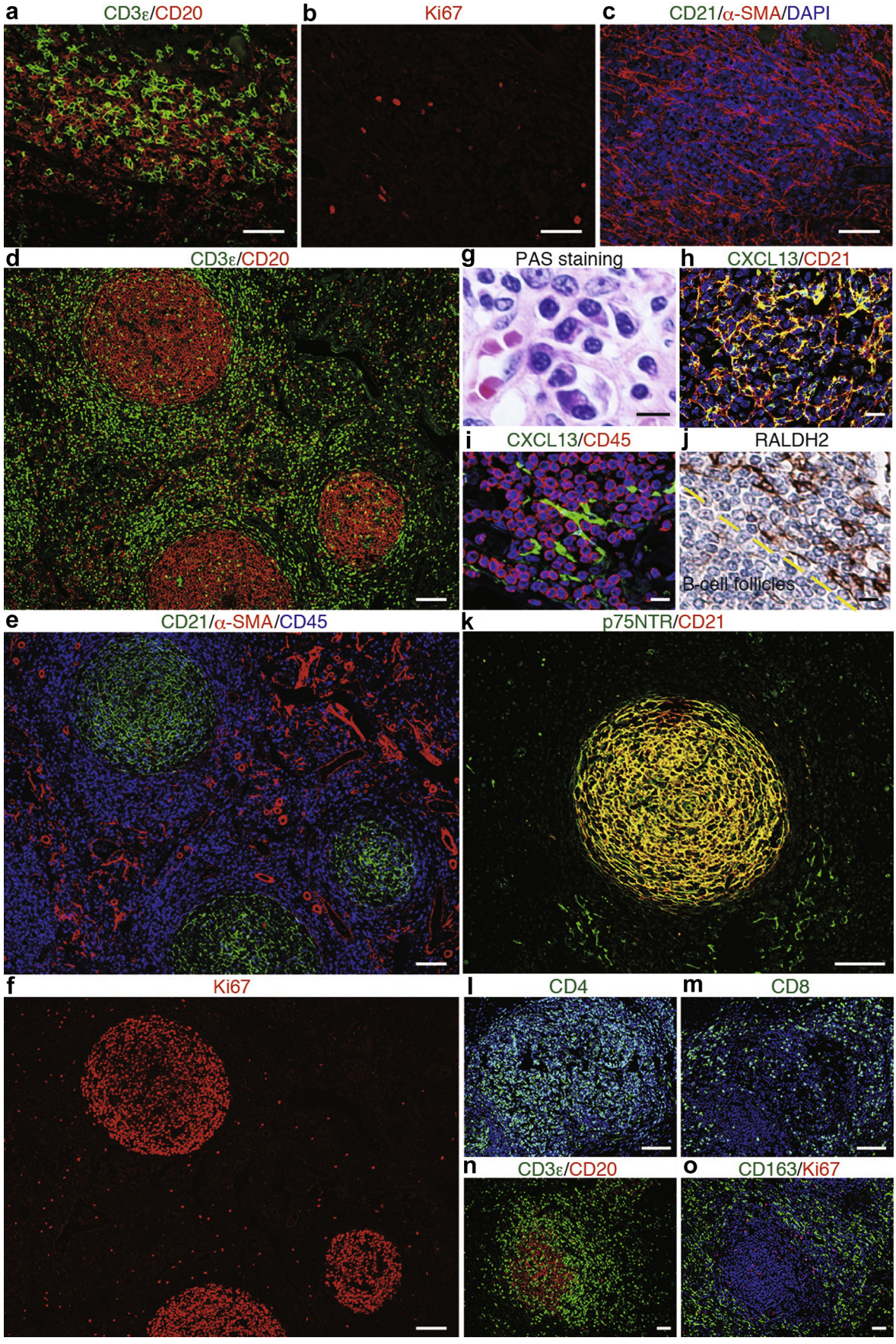
a
CD3ε/CD20
b
Ki67
c
CD21/α-SMA/DAPI
d
CD3ε/CD20
g
PAS staining
h
CXCL13/CD21
i
CXCL13/CD45
j
RALDH2
B-cell follicles
e
CD21/α-SMA/CD45
k
p75NTR/CD21
f
Ki67
l
CD4
m
CD8
n
CD3ε/CD20
o
CD163/Ki67

lymphoid organs, which correspond to the sites of B-cell proliferation and hypermutation, and of antigen-driven selection, respectively.[23]

TLT classification into 3 stages based on the presence of FDCs and germinal centers

Phenotypic analysis of TLTs revealed that TLTs could be classified into distinct phenotypes, based on the presence of CD21-positive FDCs, and germinal centers, in other words, dense Ki67-positive B-cell clusters, within TLTs (Figure 3a–c). TLTs containing neither FDCs nor germinal centers were defined as stage I TLTs, whereas TLTs that contain FDCs but lack germinal centers were defined as stage II TLTs. TLTs with prominent FDCs and germinal centers were defined as stage III. Stage I TLTs were composed of mixed T- and B-cell aggregates, while stage II or III TLTs were composed of B-cell clusters, surrounded by T cells (Figure 3b). Whereas scattered Ki67-positive cells were detected in FDC network areas in stage II TLTs, Ki67-positive cell clusters, in other words, germinal centers, were detected in those with stage III TLTs (Figure 3a).

In stage III TLT, we found a unique subpopulation of fibroblasts just around FDCs, which was negative for α-SMA and CD21 (Figure 3d) but positive for CXCL13 (Figure 3e). This unique localization and intermediate phenotype suggested the existence of fibroblasts with a transitional property between myofibroblasts and FDCs, which were reminiscence of pre-FDCs in the spleen.[24]

TLTs and lymphocyte infiltration are distinguishable in their cellular composition and functional potential for lymphocyte activation

Although TLTs in advanced stages, which contain FDCs, are easily distinguishable from lymphocyte infiltration, the identification of early stage TLTs requires more accurate characterization. Immunostaining of CD3ε and B220 of aged injured kidneys showed that T lymphocytes were observed broadly in renal parenchyma (Figure 4a and b), whereas B lymphocytes were almost exclusively present within and just around TLTs (Figure 4a and b), consistent with the observation in TLTs in tumor microenvironment[25] and chronically rejected transplanted organs.[13] Quantitative analysis of the number of T and B cells in the interstitium with or without stage I TLTs in aged injured kidney revealed that B cell–T cell ratios were remarkably higher in stage I TLTs compared with those in lymphocyte infiltration (Figure 4c). Because B cells are recruited mainly by CXCL13, a powerful driving force for B-cell recruitment,[4] we stained CXCL13 and confirmed that CXCL13 was exclusively expressed within TLTs and were detected in most of the stage I TLTs in aged injured kidneys (Figure 4d and e), which is consistent with our previous study.[10] These results suggest that the difference in B cell–T cell ratios between stage I TLTs and lymphocyte infiltration could be derived from the exclusive expression of CXCL13 within TLTs. In addition, we also confirmed that stage I TLTs contained many proliferating lymphocytes (Figure 4f and g). We also analyzed stage I TLTs and lymphocyte infiltration in human kidneys and confirmed higher B cell–T cell ratios, presence of proliferating lymphocytes, and CXCL13 expression in stage I TLTs (Figure 4h–n), although, unlike mouse stage I TLTs, stage I TLTs containing CXCL13 signals were not so frequent in human kidneys. Taken together, stage I TLTs and lymphocyte infiltration are clearly distinguishable by their cellular composition and functional potential for lymphocyte activation. A B-cell cluster is a defining characteristic of TLTs and is sufficient for identifying TLTs.

TLT stages reflect the severity of kidney injury in murine kidneys

To better understand the relation between TLT stage and renal damages, we used our murine model inducing renal TLTs. In our previous study, we showed that 12-month-old mice exhibited multiple TLTs after ischemic reperfusion injury (IRI) in an ischemia time-dependent manner.[10] TLTs expanded and occupied larger areas of renal parenchyma as the time after IRI increased.

We now defined and classified mouse TLTs based on our staging of human TLTs (Figure 5a). In parallel to the expansion of TLTs, the numbers of total TLTs consistently increased over time after IRI (Figure 5b; Supplementary Table S2A) and the number and proportion of advanced-stage TLTs (stage II and III TLTs) consistently increased over time after IRI (Figure 5c–e; Supplementary Table S2B and C), indicating that TLT stage reflects developmental stage of TLTs. The total TLT numbers, advanced-stage TLT numbers, and the proportion of advanced-stage TLTs were also higher in kidneys with 45-minute IRI than in those with 30-minute IRI (Figure 5f–i; Supplementary Table S2D–F), suggesting the potential of TLT stage as a marker for kidney injury and inflammation. In our previous study, we showed that 23-month-old mice develop TLT spontaneously without injury.[10] Here we noted that total TLT numbers as well as the numbers of advanced TLTs in 23-month-old mice were smaller than those in IRI-induced models (Figure 5f–h;

Figure 2 | Cellular and molecular components of tertiary lymphoid tissue in pyelonephritic kidneys. Immunohistochemical analysis of human pyelonephritic kidneys. Immunofluorescence of (**a**) CD3ε (a T-cell marker) and CD20 (a B-cell marker); (**b**) Ki67; (**c**) CD21 (a follicular dendritic cell marker), α-smooth muscle actin (α-SMA), and 4′,6-diamidino-2-phenylindole (DAPI); (**d**) CD3ε and CD20; (**e**) CD21, α-SMA, and CD45; (**f**) Ki67; (**h**) CXC chemokine ligand 13 ([CXCL13], a homeostatic chemokine) and CD21; (**i**) CXCL13 and CD45; (**k**) p75 neurotrophin receptor ([p75NTR], a neural crest marker) and CD21; (**l**) CD4; (**m**) CD8; (**n**) CD3ε and CD20; and (**o**) CD163 (a macrophage marker) and Ki67. (**g**) Periodic acid–Schiff (PAS) staining of plasma cells. (**j**) Immunohistochemical analysis of retinalaldehyde dehydrogenase 2 (RALDH2). Parts (**a–c**), (**d–f**), (**l,m**), and (**n,o**) are serial sections. (**j**) The yellow dotted line indicates the border of B-cell follicles. Bars = (**d–f,k–m**) 100 μm, (**a–c,j,n–o**) 50 μm, and (**g–i**) 10 μm. To optimize viewing of this image, please see the online version of this article at www.kidney-international.org.

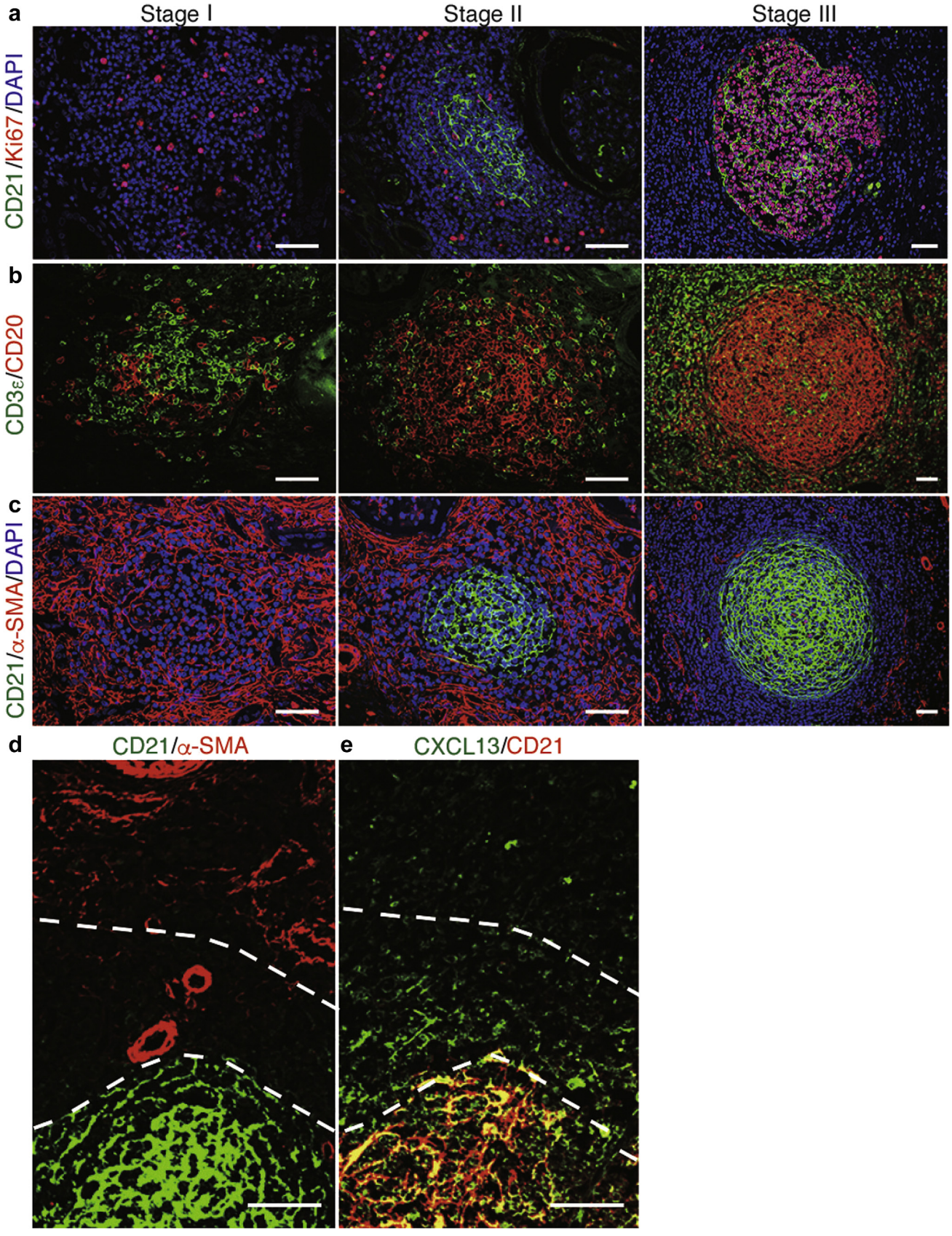
a
Stage I
Stage II
Stage III
CD21/Ki67/DAPI
b
CD3ε/CD20
c
CD21/α-SMA/DAPI
d
CD21/α-SMA
e
CXCL13/CD21

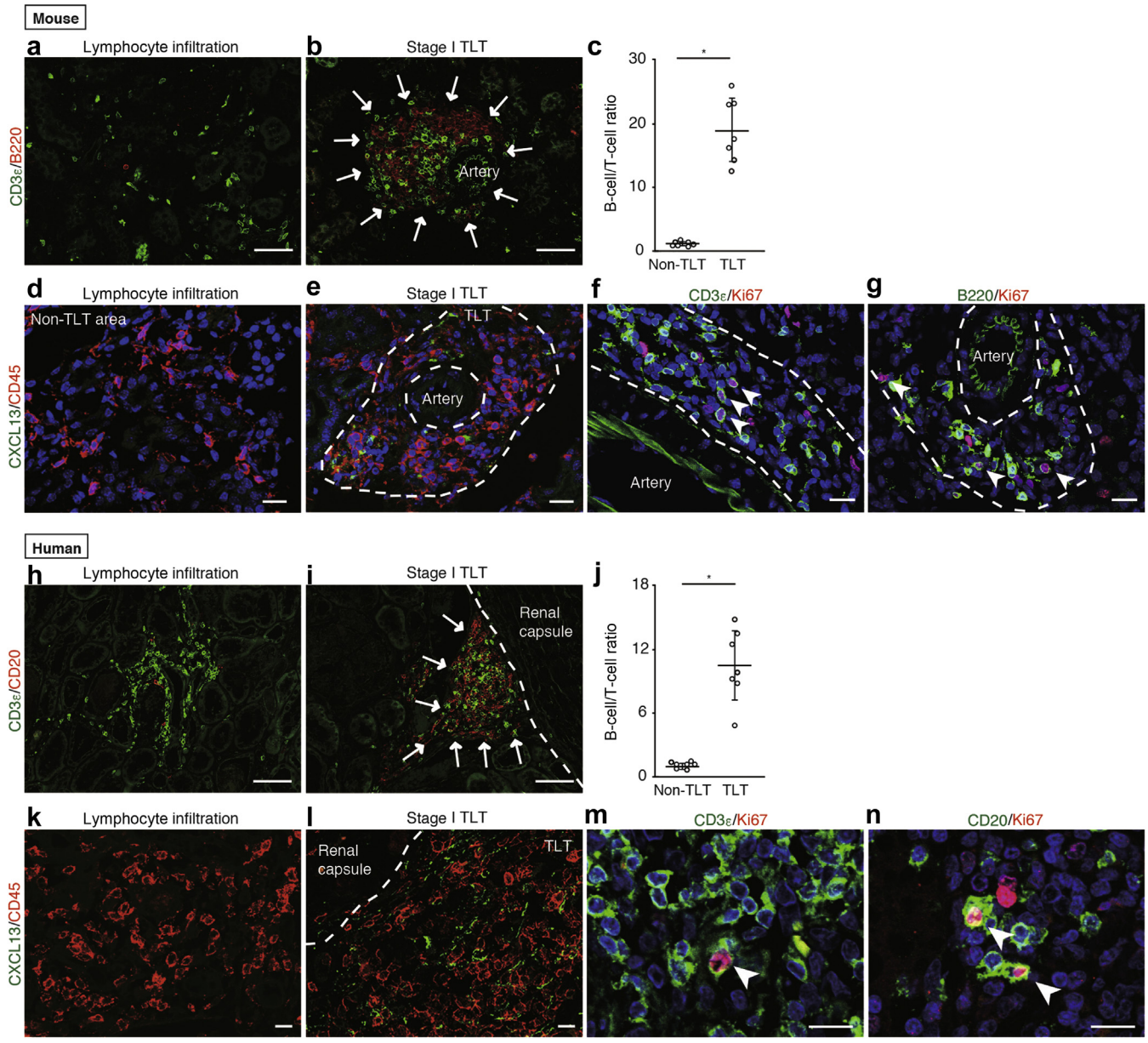

Figure 4 | Stage I tertiary lymphoid tissues (TLTs) were distinct from lymphocyte infiltration. Immunofluorescence of stage I TLTs and lymphocyte infiltration in murine and human kidneys. (**a–g**) Analysis of stage I TLTs and lymphocyte infiltration in aged injured kidneys in mice. Immunofluorescence of (**a,b**) CD3ε (a T-cell marker) and B220 (a B-cell marker); (**d,e**) CXC chemokine ligand 13 ([CXCL13], a homeostatic chemokine), CD45, and 4′,6-diamidino-2-phenylindole (DAPI) in lymphocyte infiltration and stage I TLTs 8 and 24 days after 45-minute ischemic reperfusion injury in 12-month-old mice. (**f,g**) Immunofluorescence of (**f**) CD3ε, Ki67, and DAPI, and (**g**) B220, Ki67, and DAPI in stage I TLTs. (**c**) B cell–T cell ratio in stage I TLTs (TLT) and lymphocyte infiltration (non-TLT) ($n = 7$ per group), calculated by dividing the numbers of B cells by the numbers of T cells in each area. (**h–n**) Analysis of stage I TLTs and lymphocyte infiltration in aged and pyelonephritis human kidneys. Immunofluorescence of (**h,i**) CD3ε and CD20; (**k,l**) CXCL13 and CD45 in stage I TLTs and lymphocyte infiltration. (**m,n**) Immunofluorescence of (**m**) CD3ε, Ki67, and DAPI, and (**n**) CD20, Ki67, and DAPI in stage I TLTs. (**j**) B cell–T cell ratio in stage I TLTs (TLT) and lymphocyte infiltration (non-TLT) ($n = 7$ per group) in human kidneys. (**b,i**) The white arrows indicate the localization of TLTs, and the white arrowheads are (**f,m**) proliferating T cells and (**g,n**) proliferating B cells. The white dotted lines indicate the border of (**e–g**) stage I TLTs and (**i,l**) renal capsules. (**c,j**) Values are means ± SD. (**c,j**) A 2-tailed Student's *t* test was used to analyze data. $^*P < 0.01$. Bars = (**a,b**) 50 μm, (**d–g,k–n**) 10 μm, and (**h,i**) 100 μm. To optimize viewing of this image, please see the online version of this article at www.kidney-international.org.

Figure 3 | Tertiary lymphoid tissues were classified into 3 stages based on the presence of follicular dendritic cells and germinal centers. Representative immunofluorescence micrographs of 3 distinct stages (I, II, III) of tertiary lymphoid tissues in human kidneys. Immunofluorescence of (**a**) CD21 (a follicular dendritic cell marker), Ki67 (a cell proliferation marker), and 4′,6-diamidino-2-phenylindole (DAPI); (**b**) CD3ε (a T-cell marker) and CD20 (a B-cell marker); and (**c**) CD21, α-smooth muscle actin (α-SMA), and DAPI. (**b,c**) Each stage is a serial section. Immunofluorescence of (**d**) CD21 and α-SMA and (**e**) CXC chemokine ligand 13 (CXCL13) and CD21 (serial sections). (**d,e**) The white dotted lines indicate the border of the CD21/α-SMA–double negative zone. Bars = 50 μm. To optimize viewing of this image, please see the online version of this article at www.kidney-international.org.

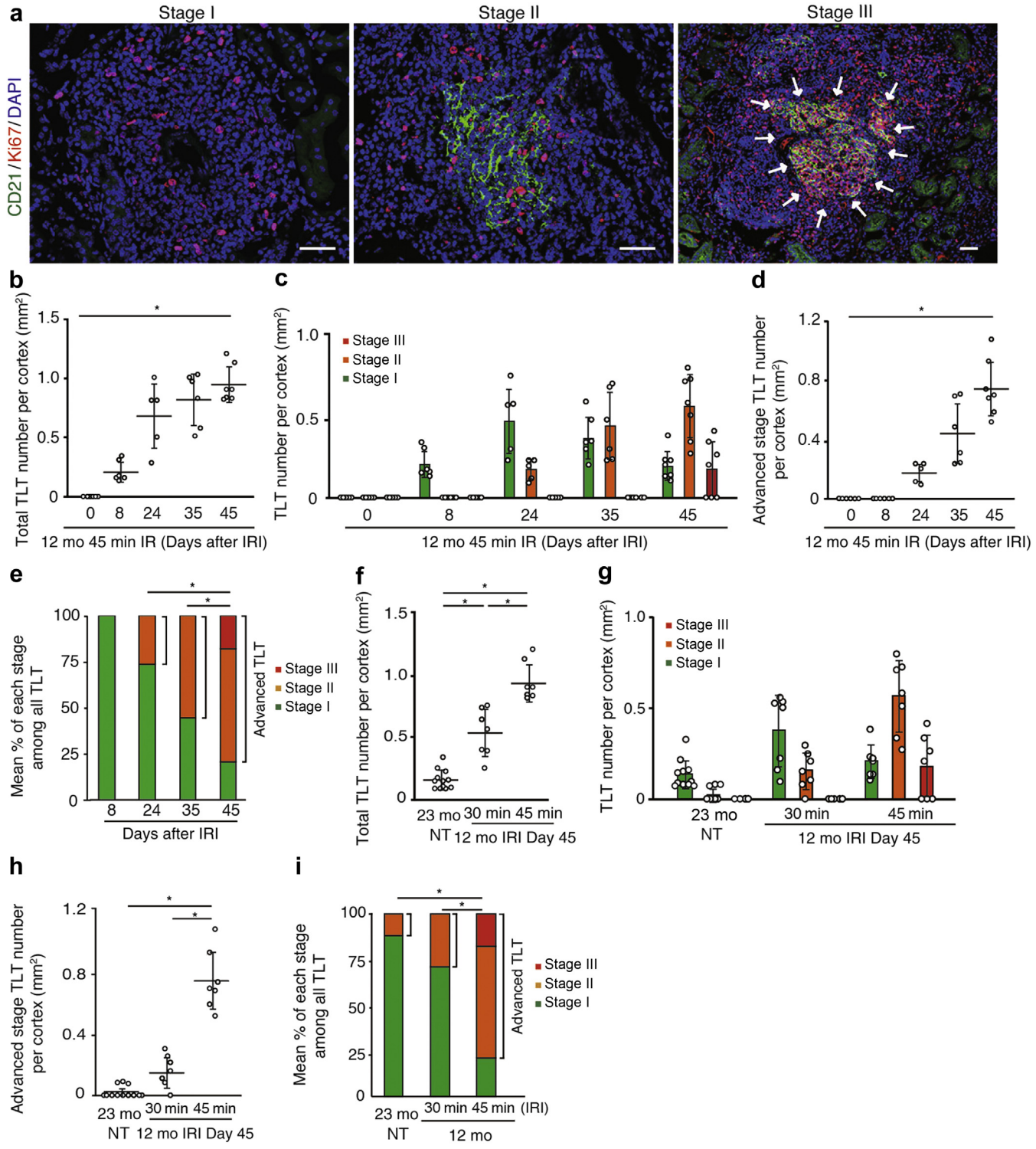

Figure 5 | The developmental stage of tertiary lymphoid tissues (TLTs) was associated with the severity of kidney injury in mice. (**a**) Histologic analysis of aged injured kidneys in mice. Immunofluorescence of CD21 and Ki67 shows 3 types of TLTs in aged injured kidneys. White arrows indicate the localization of the germinal center. (**b–g**) Quantification of the TLT numbers and stages in aged mouse kidneys. Number of (**b**) total TLTs; (**c**) stage I, II, and III TLTs; and (**d**) advanced-stage TLTs; as well as (**e**) the proportion of stage I, II, and III TLTs at various time points after 45-minute ischemic reperfusion injury (IRI) in 12-month-old mice (days 0 and 8: $n = 6$, day 24: $n = 5$, day 35: $n = 6$, day 45: $n = 7$). (**d**) The numbers of advanced-stage TLTs (stage II and III TLT) significantly increased over time after IRI ($P < 0.01$) (Supplementary Table S2B). The number of (**f**) total TLTs; (**g**) stage I, II, and III TLTs; and (**h**) advanced-stage TLTs; as well as (**i**) the proportions of stage I, II, and III TLTs in 23-month-old mouse kidneys without injury ($n = 12$), and 12-month-old mouse kidneys 45 days after 30-minute ($n = 7$) or 45-minute ($n = 7$) IRI. (**h**) The numbers of advanced-stage TLTs in 45-minute IRI were significantly higher than those of 30-minute IRI and 23-month-old mouse kidneys ($P < 0.01$) (Supplementary Table S2E). (**b–d,f–h**) Values are means ± SD. Data were analyzed using (**b,d**) (continued)

Supplementary Table S2D) and 88% of these TLTs in 23-month-old mice were in stage I (Figure 5i). The difference in total TLT numbers and advanced-stage TLT numbers between 23-month-old mouse kidneys and 45-minute IRI kidneys was 0.80 per mm^2 (95% confidential interval [CI], 0.66–0.93) and 0.72 per mm^2 (95% CI, 0.61–0.84), respectively (Supplementary Table S2D and E).

TLT stages are reversible in murine kidneys

To investigate whether TLT stages can regress, we administered dexamethasone (Dex) from 35 days after an ischemic insult (Figure 6a), when TLTs at stage I and II are already established (Figure 5c–e). Ten days later, the kidneys of Dex-treated mice exhibited significantly smaller TLTs (Figure 6b and c) at less advanced stages (Figure 6e-g; Supplementary Table S3B and C) than those at day 35, although the total numbers of TLTs were not statistically different among day 35, day 45, and day 45 treated with Dex (Figure 6d; Supplementary Table S3A). Consistent with this, the expression of homeostatic chemokines, proinflammatory cytokines, and fibrosis markers was also significantly reduced in Dex-treated mice (Figure 6h), and the expression of these markers strongly correlated with TLT sizes (Figure 6i). The number of Foxp3-positive T cells and the expression levels of Foxp3 were also reduced in Dex-treated mice (Supplementary Figure S8A and B).

Dex treatment suppressed TLT formation and improved renal function with fibrosis resolution in murine adenine nephropathy

To investigate whether TLT resolutions are accompanied with the improvement in renal function, we induced adenine nephropathy model in aged wild-type mice and administered either Dex or vehicle from 12 days after the initiation of adenine diet feeding (Figure 7a). Twenty-one days after disease induction and 9 days of treatment, aged vehicle-treated mice exhibited several advanced TLTs and renal dysfunction (Figure 7b–h). Treatment with Dex fully abolished the formation of TLTs and led to significantly improved renal function compared with that of vehicle-treated mice (Figure 7b–h). Consistent with this, the expressions of homeostatic chemokines *Cxcl13* and *Ccl19* and proinflammatory cytokines were significantly reduced in Dex-treated mice (Figure 7i). Renal fibrosis score, which was quantified as α-SMA-positive area in the renal interstitial space, and the expression of fibrosis markers such as *Col1a1* and *Fn1* were also improved in Dex-treated mice (Figure 7j–l).

TLT stages in aged and pyelonephritic human kidneys

Finally, we examined the developmental stages of renal TLTs in aged patients and patients with chronic pyelonephritis ($n = 69$ and $n = 16$, respectively). In this study, CKD were defined as either estimated glomerular filtration rate (eGFR) < 60 ml/min per 1.73 m^2 or positive urinary protein. The clinical characteristics evaluated in this study are summarized in Tables 1 and 2. Whereas 47.8% of aged patients exhibited TLTs, all patients with pyelonephritis exhibited TLTs (Figure 8a). Among patients with TLTs, patients with pyelonephritis, compared with aged patients, exhibited significantly higher numbers of total TLTs and advanced-stage TLTs and a higher proportion of advanced-stage TLTs (Figure 8b–e; Supplementary Table S4A–C). The difference in total TLT numbers between aged kidneys and pyelonephritic kidneys was 0.22 per mm^2 (95% CI, 0.16–0.28) (Supplementary Table S4A). To compare renal TLTs related to aging alone and those driven by kidney injury, we further classified the aged patients into 2 groups: aged patients with or without CKD ($n = 29$ and $n = 40$, respectively). TLTs were detectable in the kidneys of 43% of patients without CKD and 55% of those with CKD (Figure 8f). Consistent with the results in mice, almost 90% of renal TLTs in aged patients without CKD were stage I TLTs. Among aged patients with TLTs, patients with CKD, compared with patients without CKD, exhibited significantly higher numbers of total TLTs and advanced-stage TLTs and a hhigher proportion of advanced-stage TLTs (Figure 8g–j and Supplementary Table S4D–F). Among aged patients with renal TLTs, the numbers of total and advanced-stage TLTs as well as the proportion of advanced-stage TLTs were not statistically different between aged patients in the presence or absence of proteinuria or a reduced GFR (eGFR < 60 ml/min per 1.73 m^2) (Supplementary Figure S9).

DISCUSSION

In the present study, we analyzed surgically resected human pyelonephritis kidneys and found multiple heterogeneous TLTs, which gave us a unique opportunity to comprehensively understand TLTs in human kidneys. To our knowledge, this is the first study to demonstrate an association between the developmental stage of TLT and kidney injury in mice and humans from 2 independent cohorts, supporting the potential of TLT stage as a marker reflecting local injury and inflammation. Additionally, we showed that TLT stages decreased with Dex treatment accompanied with improvement of renal inflammation, indicating the reversibility of TLT stages. Furthermore, we have shown that the administration of Dex suppressed TLT formation and improved renal function and fibrosis. Moreover, we found spatial and developmental similarities of TLTs in patients with pyelonephritis and aged patients, indicating that TLT formation may not be disease-specific but rather a common pathological process. Although TLT development in human kidneys has been observed in several disease conditions,[10,12,13,15,26,27] the number of diseases in which renal TLTs can be observed is

Figure 5 | (continued) a trend test, (**e,i**) a generalized estimating equation, and (**f,h**) 1-way analysis of variance with Bonferroni *post hoc* analysis. The numbers of TLTs are the numbers per unit area of cortex (per mm^2). *$P < 0.01$. Bars = 50 μm. To optimize viewing of this image, please see the online version of this article at www.kidney-international.org.

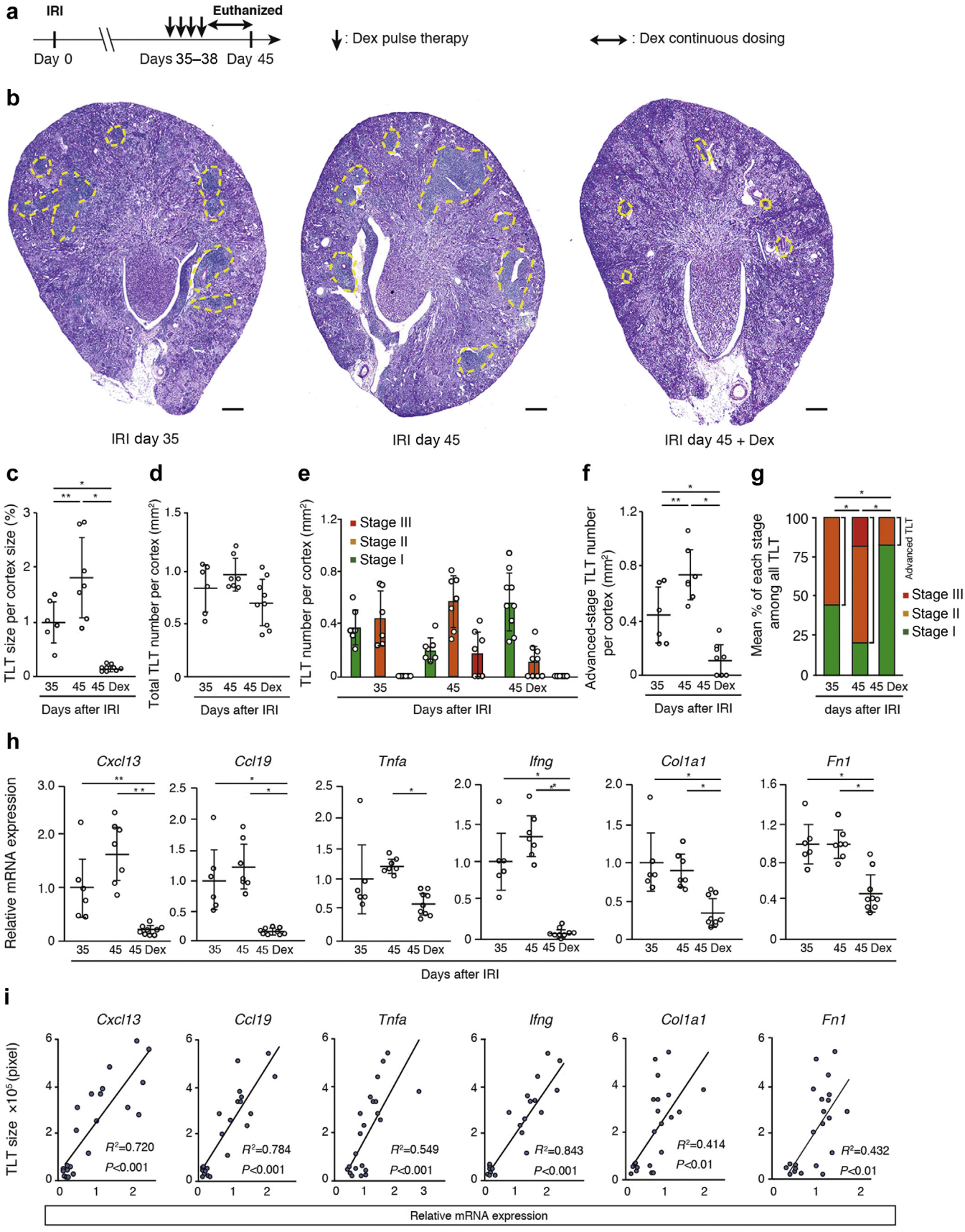
a
IRI
Euthanized
Day 0
Days 35–38
Day 45
: Dex pulse therapy
: Dex continuous dosing
b
IRI day 35
IRI day 45
IRI day 45 + Dex
c
TLT size per cortex size (%)
Days after IRI
d
Total TLT number per cortex (mm²)
Days after IRI
e
TLT number per cortex (mm²)
Stage III
Stage II
Stage I
Days after IRI
f
Advanced-stage TLT number per cortex (mm²)
Days after IRI
g
Mean % of each stage among all TLT
Advanced TLT
Stage III
Stage II
Stage I
days after IRI
h
Cxcl13
Ccl19
Tnfa
Ifng
Col1a1
Fn1
Relative mRNA expression
Days after IRI
i
Cxcl13
Ccl19
Tnfa
Ifng
Col1a1
Fn1
TLT size ×10⁵ (pixel)
R²=0.720
P<0.001
R²=0.784
P<0.001
R²=0.549
P<0.001
R²=0.843
P<0.001
R²=0.414
P<0.01
R²=0.432
P<0.01
Relative mRNA expression

predicted to increase further. Taken together, these findings provide insight into the biological features of TLTs in the kidney and implicate TLT stage as a potential inflammatory marker.

TLT is a specialized microenvironment for lymphocyte activation (Figure 9), which clearly distinguishes TLTs from simple inflammatory cell infiltration,[1–3] even in the early stage (stage I TLT). TLTs are characterized by distinct phenotypic fibroblasts within TLT, which produce homeostatic chemokines such as CXCL13.[10,11,28] Consistently, the T cell–B cell ratio clearly distinguished stage I TLTs from lymphocyte infiltration (Figure 4a–c and h–j). Indeed, it has been previously demonstrated that, whereas infiltrating T cells are broadly detectable across the organs, infiltrating B cells are almost exclusively detectable in the form of TLTs in tumor microenvironment,[25] as well as in chronically rejected transplanted kidneys.[13]

A sustained overproduction of proinflammatory cytokines by lymphocytes activated in TLTs has been implicated as a primary reason why inflammation fails to resolve in various tissues.[1–3,29] In addition, autoantibody production in TLTs has been demonstrated to contribute to local pathology.[30] Finally, unlike lymph nodes, TLTs are not encapsulated, and thus can markedly expand in the renal interstitial compartment and occupy broad areas of the renal parenchyma. These considerations and findings suggest that TLTs play important roles in persistent inflammation and tissue destruction that characterize kidney disease progression. Alternatively, TLTs also can play immunoregulatory roles.[31] In the murine atherosclerosis model, for instance, TLTs convert naïve T cells into induced Foxp3-positive regulatory T cells and control chronic inflammation.[32] In this study, Foxp3-positive regulatory T cells were detectable within TLTs (Supplementary Figures S6 and S8), though the numbers were not relatively large, and decreased after Dex treatment (Supplementary Figure S8). Therefore, TLTs can enforce or attenuate chronic inflammation and the balance is context-dependent.

The frequency and developmental stage of TLTs might be distinct for each underlying kidney disease. In this study, we showed that the incidence of TLTs was 100% in patients with chronic pyelonephritis, whereas only about 50% of aged patients developed TLTs. Additionally, we found a large difference in total and advanced-stage TLT numbers between aged kidneys and pyelonephritic kidneys. In TLTs driven by infections, such as inducible bronchus-associated lymphoid tissue, the occurrence, size, and number depend on the type and duration of antigenic exposure.[33,34] In the present study, all patients with pyelonephritis had severe disease refractory to medications and had to undergo nephrectomy, indicating long-time antigen exposure that explains the high frequency and advanced stages of TLTs in these patients.

The frequency of TLTs in aged kidneys in this study (around 50%) was higher than that in our previous report (28%).[10] This difference likely results from different definitions of TLTs. In our previous study, we defined TLTs as inflammatory cell aggregates containing CXCL13- and Ki67-positive cells,[10] while in this study we defined TLTs as organized lymphocyte aggregates with signs of proliferation. Most studies have defined TLTs as organized lymphocyte aggregates. Additionally, CXCL13 is not constitutively detectable by immunostaining due to the limitation of sensitivity even in FDCs in secondary lymphoid organs,[35] which may lead to an underestimation of the TLT frequency in our previous study. Our finding that TLTs occur in up to 50% of aged patients is also of interest given that, Furman *et al.*[36] have recently reported that the elderly patients can be stratified based on the expression of inflammasome genes, into an inflammatory and noninflammatory aged patient group. It remains to be proven whether an inflammatory background of the host may indeed predispose to TLT formation in human aged kidneys.

An important component in this study was to use a murine model of renal TLTs to assess the temporal relationship between TLT development and tissue damage. We demonstrated that the severity of kidney injury determined by ischemia time affected TLT development. These findings were also supported by experimental evidence showing that the induction of TLTs was dependent, at least partly, on the expression levels of inflammatory cytokines such as tumor necrosis factor-α and lymphotoxin.[13,24] We therefore speculate that the heterogeneity of TLTs in human kidneys, as described, may relate to the variable severity of injury. Interestingly, most of the age-dependent spontaneous TLTs in mice are stage I TLTs, suggesting that aging alone is not sufficient, and massive cell death is required for driving more advanced-stage TLTs. Additionally, we showed that even advanced-stage TLTs can respond to Dex treatment, shrink, and revert to less advanced stages in the murine model. This result indicates that therapeutic approaches to reverse TLT

Figure 6 | The developmental stages of tertiary lymphoid tissues (TLTs) were reversible with the treatment of dexamethasone (Dex) in mice. Quantification of TLT numbers and stages of 12-month-old mouse kidneys at 45 days after 45-minute ischemic reperfusion injury (IRI) treated with Dex from day 35 (45 Dex) ($n = 9$). (**a**) Experimental protocol; (**b**) periodic acid–Schiff staining; (**c**) cumulative TLT sizes per cortex; (**d**) total TLT numbers; (**e**) stage I, II, and III TLT numbers; (**f**) advanced TLT numbers; and (**g**) the proportion of stage I, II, and III TLTs in 12-month-old mouse kidneys 35 and 45 days after 45-minute IRI (day 35: $n = 6$, day 45: $n = 7$ per group), and 12-month-old mouse kidneys 45 days after 45-minute IRI treated with Dex from day 35 (45 Dex) ($n = 9$). (**h**) *Cxcl13*, *Ccl19* (a homeostatic chemokine), *Tnfa*, *Ifng*, *Col1a1*, and *Fn1* mRNA levels in the IRI kidneys, and (**i**) their associations with TLT sizes (35: aged kidneys 35 days after 45-minute IRI; 45: aged kidneys 45 days after 45-minute IRI; 45 Dex: aged kidneys treated with Dex from days 35–45). (**b**) Yellow dash lines indicate the localization of TLT. (**c**) The TLT sizes were expressed relative to those of aged IRI kidneys 35 days after 45-minute IRI. The expression levels of mRNA were normalized to those of *Gapdh* and expressed relative to those of aged IRI kidneys 35 days after IRI. Reverse transcriptase polymerase chain reaction primer sequences are listed in Supplementary Table S5. (**c–f,h**) Values are means ± SD. Data were analyzed using (**c,d,f–h**) 1-way analysis of variance with Bonferroni *post hoc* analysis and (**g**) a generalized estimating equation. The number of TLTs was shown as the numbers per unit area of cortex (per mm^2). *$P < 0.01$; **$P < 0.05$. (**i**) Correlation was determined by Pearson's correlation analysis. Bars = 300 μm. To optimize viewing of this image, please see the online version of this article at www.kidney-international.org.

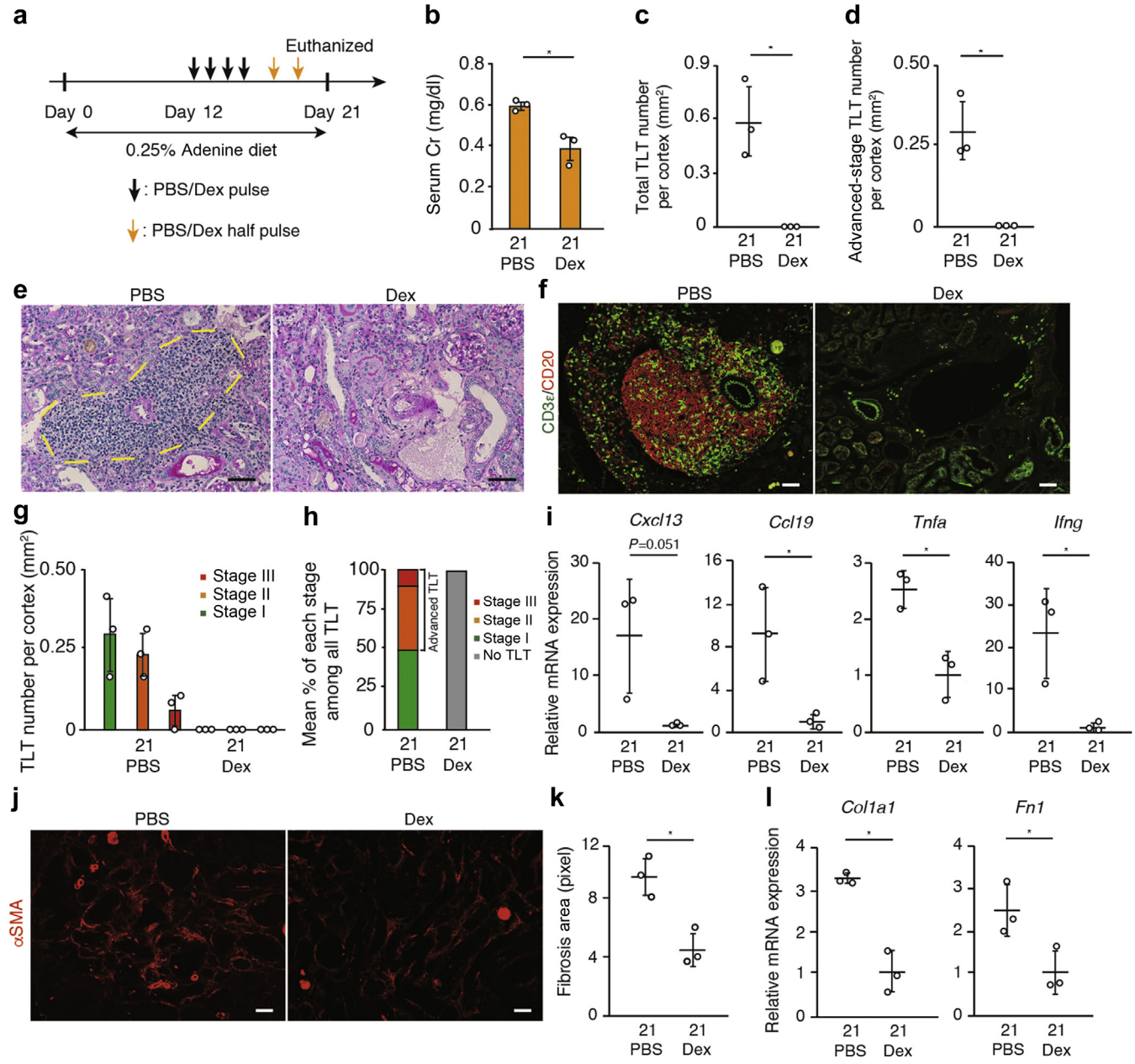

Figure 7 | Dexamethasone (Dex) treatment abolished tertiary lymphoid tissue (TLT) formation and improved renal function as well as fibrosis in murine adenine nephropathy model. (**a**) Experimental protocol for parts (**b–l**) (n = 3–4 in each group). Dex treatment abolished TLT formation and improved renal function as well as renal fibrosis in 10-month-old female mice subjected to 0.25% adenine nephropathy models as shown by (**b**) serum creatinine (Cr) levels; (**c**) total TLT numbers; (**d**) advanced-stage TLT numbers; (**e**) periodic acid–Schiff staining; (**f**) immunofluorescence of CD3ε (a T-cell marker) and CD20; (**g**) stage I, II, and III TLT numbers; (**h**) the proportion of stage I, II, and III TLTs among all TLTs; (**i**) *Cxcl13*, *Ccl19* (a homeostatic chemokine), *Tnfa,* and *Ifng* mRNA levels; (**j**) immunofluorescence of α-smooth muscle actin (α-SMA); (**k**) fibrosis area; and (**l**) *Col1a1* and *Fn1* mRNA levels. (**b–d,g,i,k–l**) Values are means ± SD. (**e**) Yellow dash lines indicate the localization of TLT. Bars = 50 μm. (**i,l**) The expression levels of mRNA were normalized to those of *Gapdh* and expressed relative to those of Dex-treated kidneys. The numbers of TLTs are the numbers per unit area of cortex (per mm^2). Reverse transcriptase polymerase chain reaction primer sequences are listed in Supplementary Table S5. (**b–d,i,k,l**) Data were analyzed using 2-tailed Student's t test. *$P < 0.01$. PBS, phosphate-buffered saline. To optimize viewing of this image, please see the online version of this article at www.kidney-international.org.

stages could be promising to attenuate intrarenal aberrant inflammation. Given that renal biopsy is an invasive procedure and might not be sufficient to representatively reflect renal TLTs, biomarkers reflecting TLT stages should ideally be invented. Further molecular insights into the TLT stages are required to yield specific biomarkers reflecting TLT development.

We found a unique subpopulation of fibroblasts around the FDC-harboring germinal center (Figures 3 and 9). These fibroblasts were characterized by their specific localization and

Table 2 | Clinical characteristics of aged Japanese patients evaluated in the study

	Total	CKD−	CKD+	TLT−	TLT+
Aged patients (*n*)	69	40	29	36	33
Age (yr)					
Average	70.8	69.7	72.2	70.1	71.5
Median	70.0	69.0	72.0	68.0	71.0
Range	60.0–89.0	60.0–85.0	62.0–89.0	60.0–85.0	60.0–89.0
Sex (*n*)					
Male	34	20	14	19	15
Female	35	20	15	17	18
Renal function					
Serum Cr (mg/dl)					
Average	0.81	0.71	0.95[a]	0.78	0.84
Median	0.75	0.68	0.93	0.72	0.80
Range	0.40–1.53	0.40–0.95	0.50–1.53	0.50–1.53	0.40–1.41
eGFR (ml/min per 1.73 m^2)					
Average	66.1	73.9	55.4[a]	67.9	64.1
Median	64.1	70.2	53.5	64.7	62.6
Range	29.3–116.5	60.2–114.0	29.3–116.5	35.7–99.0	29.3–116.5
Complication					
DM (+, %)	20.0	15.0	27.6[b]	19.4	21.2
HTN (+, %)	62.3	55.0	72.4[b]	58.3	66.6

CKD, chronic kidney disease; Cr, creatinine; DM, diabetes mellitus; eGFR, estimated glomerular filtration rate; HTN, hypertension; TLT, tertiary lymphoid tissues.
CKD was defined either as eGFR < 60 ml/min or positive urinary protein, which was defined as more than 1+ in urine dipstick test. Patients with HTN were defined as those with a blood pressure of 140/90 mm Hg or above. eGFR was calculated using the following formula: eGFR (ml/min per 1.73 m^2) = 194 × Cr − 1.094 × Age − 0.287 (in case of female, × 0.739).
[a]$P < 0.001$ vs. aged patients without CKD. *P* values in comparison of serum Cr and eGFR were calculated using a 2-tailed Student's *t* test, while *P* values in comparison of proportion of DM and HTN complication were calculated using Pearson's chi-squared test.
[b]Not significant.

intermediate phenotype between myofibroblasts and FDCs. Similar stromal cells have been detected in the spleen and are called pre-FDC because they are interconnected with FDC and possess some FDC-like phenotypes such as the ability to produce CXCL13, but they lack CD21 expression.[24] The fibroblast subpopulation identified in this study met the above-mentioned definition of pre-FDC (Figure 9). Further study is required to determine their function and relevance in TLT formation.

An interesting observation in our study was that TLT developed around perivascular and subcapsular areas in human kidneys irrespective of the etiology. This is consistent with our previous finding that TLTs formed around the perivascular area in murine kidney[10] and a previous report[24] showing that FDCs in the spleen developed from perivascular precursors were positive for platelet-derived growth factor receptor-β and were of stromal cell origin. These locations are the areas rich in lymphatic vessels, and further study is needed to determine the mechanism by which TLT develops exclusively in these specific areas.

This study has several limitations. First, our results provided snapshots of different phenotypic TLTs in human kidneys. However, in support of our hypothesis, we confirmed a multistep TLT development in parallel to phenotypic diversification of resident fibroblasts in mice (Figure 5a). Second, there was a possibility of underestimation of TLT stages with the use of only 2 serial sections. Nevertheless, we obtained consistent results in the relation between TLT stage and kidney injury from murine models and 2 independent human cohorts. Analysis of a large number of TLTs may compensate for errors in TLT staging. Finally, although the nephrectomy samples due to renal cell carcinoma (RCC) that were examined in this study were free of cancer, the possibility that the cancer environment contributed to the development of TLTs cannot be completely excluded.

In summary, we found the heterogeneity of TLTs in the kidney and demonstrated an association between the developmental stages of TLTs and the severity of kidney injury. Our data also might shed new light on TLT biology in the kidney and provide a further rationale for studying TLT formation as a potential inflammatory marker as well as therapeutic target in various kidney diseases.

METHODS

For detailed methods, please see the Supplementary Methods.

Analysis of human kidney specimens

All human specimens were procured and analyzed after informed consent and with approval of the ethics committee at Kyoto University Hospital and Rhenish-Westphalian Technical University of Aachen Hospitals. Kidneys from aged patients with RCC who underwent nephrectomy at Kyoto University Hospital (Kyoto, Japan) and from patients with chronic pyelonephritis who underwent nephrectomy at Rhenish-Westphalian Technical University of Aachen Hospitals (Aachen, German) were analyzed. We defined aged patients as those 60 years and older. Experienced pathologists confirmed that all of the RCC nephrectomy samples analyzed in this study were free of carcinoma. Because TLTs can develop as a result of certain diseases, patients who had a clinical history or laboratory evidence or both of the following diseases were excluded from the analysis of the aged kidney samples from Kyoto University Hospitals: (i) pyelonephritis; (ii) glomerulonephritis; (iii) autoimmune kidney disease; (iv) graft rejection; (v) end-stage renal diseases; and (vi) hematological malignancies.

For the quantitative analysis of TLT formation frequency, kidneys from 69 aged patients with RCC who underwent nephrectomy at Kyoto University Hospital and from 16 patients with chronic pyelonephritis who underwent nephrectomy at University Clinic of Rhenish-Westphalian Technical University of Aachen were analyzed. Clinical data including medical history, complications, and laboratory data are presented in Tables 1 and 2. CKD were defined as either eGFR < 60 ml/min per 1.73 m^2 or positive urinary protein. We defined proteinuria positive as more than 1+ in urine dipstick test. Among 69 aged patients with RCC, 29 patients had CKD including nephrosclerosis and diabetic kidney disease. In total, 10 aged patients exhibited proteinuria and 59 aged patients did not; 44 patients exhibited eGFR > 60 ml/min per 1.73 m^2 and 25 patients exhibited eGFR < 60 ml/min per 1.73 m^2. Although all the samples of nephrectomies were diagnosed by nephropathologists as pyelonephritis, and despite the indication of nephrectomies in our centers, the possibility of uncertainty as to the clinical diagnoses cannot be excluded.

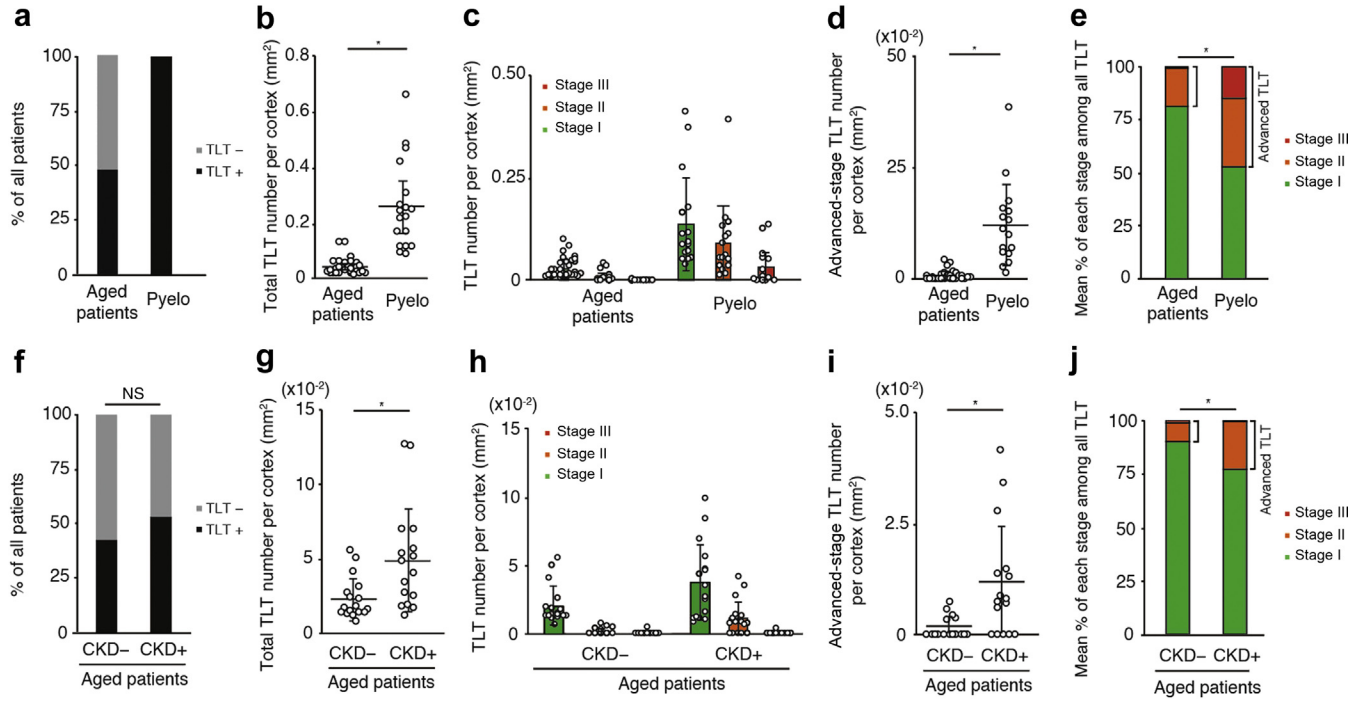

Figure 8 | The developmental stage of tertiary lymphoid tissues (TLTs) in aged and pyelonephritic (Pyelo) human kidneys. (**a–d**) Quantification of TLTs in aged and Pyelo human kidneys. (**a**) Relative frequencies of TLT development in kidneys of aged patients ($n = 69$) and patients with pyelonephritis ($n = 16$). (**b–e**) Quantification of TLTs in aged patients and patients with pyelonephritis with renal TLTs ($n = 33$ and 16, respectively). (**b**) Numbers of total TLTs; (**c**) stage I, II, and III TLTs; and (**d**) advanced-stage TLTs. (**e**) The proportion of stage I, II, and III TLTs. (**f**) Relative frequencies of TLT development in aged human kidneys with or without chronic kidney disease (CKD) ($n = 29$ and 40, respectively). (**g–j**) Quantification of TLTs in aged patients with or without CKD, who exhibited renal TLTs ($n = 16$ and 17, respectively). (**g**) Numbers of total TLTs; (**h**) stage I, II, and III TLTs; and (**i**) advanced-stage TLTs. (**j**) Proportions of stage I, II, and III TLTs. (**b–d,g–i**) Values are means ± SD. Numbers of TLTs are the numbers per unit area of cortex (per mm^2). The difference was analyzed using (**b,d,g,i**) 2-tailed Student's *t* test, (**e,j**) a generalized estimating equation, and (**f**) Pearson's chi-squared test. *$P < 0.01$. NS, not significant.

Identification and quantification of TLT

In the present study, we defined TLTs as the organized lymphocyte aggregates with signs of proliferation. Identification of TLT was based on the unique localization of inflammatory cell aggregates and the presence of B-cell aggregates. Quantification of TLT number and stage in renal cortex was examined with immunofluorescence of (i) CD3ε and CD20 and (ii) Ki67 and CD21 in 2 serial sections for each individual and mouse and was assessed by an experienced renal pathologist. TLT stage determination was performed based on the presence of CD21-positive FDCs and germinal centers, in other words, dense Ki67-positive B-cell clusters, within TLTs. TLTs containing neither FDCs nor germinal centers were defined as stage I

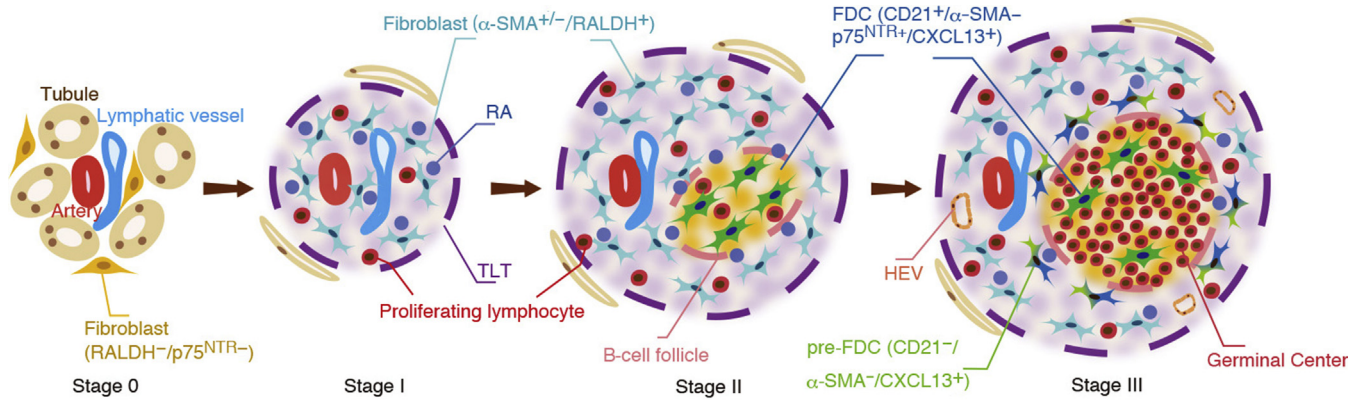

Figure 9 | Heterogeneity of tertiary lymphoid tissues (TLTs) in human kidneys. In human kidneys, TLTs appeared to develop largely through 3 distinct stages, which may represent the developmental stages. To evaluate the heterogeneity, we defined TLT stages by the presence of follicular dendritic cells (FDCs) and germinal centers, which correspond to the presumed developmental stages. α-SMA, α-smooth muscle actin; CXCL13, CXC chemokine ligand 13; HEV, high endothelial venule; p75NTR, p75 neurotrophin receptor; RA, retinoic acid; RALDH, retinaldehyde dehydrogenases 2.

TLTs, whereas TLTs that contain FDCs but lack germinal centers were defined as stage II TLTs. TLTs with prominent FDCs and germinal centers were defined as stage III. Advanced-stage TLTs were defined as TLT with FDCs (i.e., stage II and III TLTs). The numbers of TLTs were shown as the numbers per unit area of cortex (per mm^2) in mice and humans.

Animals

We utilized 12- to 13-month-old and 23-month-old C57BL6J male mice and 10-month-old C57BL6J female mice. We purchased the mice from Japan SLC (Nishi-ku Hamamatsu, Japan). Serum creatinine was measured by the creatininase–N-(3-sulfopropyl)-3-methoxy-5-methylaniline method. All mice were maintained under specific pathogen-free conditions in the animal facility at Kyoto University. All animal experiments were approved by the Animal Research Committee, Graduate School of Medicine, Kyoto University, and were conducted in accordance with the Guide for the Care and Use of Laboratory Animals (U.S. National Institutes of Health, Bethesda, MD).

DISCLOSURE

YS is employed by the TMK Project. MY is on the advisory board of Astellas and receives research grants from Astellas, Chugai, Daiichi Sankyo, Fujiyakuhin, Kyowa Hakko Kirin, Mitsubishi Tanabe, MSD, Nippon Boehringer Ingelheim, and Torii. All the other authors declared no competing interests.

ACKNOWLEDGMENTS

We thank Ms. Kasumoto, Ms. Tomita, Ms. Sakurai, Ms. Nakayama, and Ms. Ozone for their excellent technical assistance. This research was supported by the Japan Agency for Medical Research and Development (AMED) under Grants JP18gm5010002 and JP18gm0610011; partially by grants from the TMK Project, KAKENHI Grant-in-Aids for Scientific Research B (26293202, 17H04187), Grant in Aid for Scientific Research on Innovative Areas "Stem Cell Aging and Disease" (17H05642) from Ministry of Education, Culture, Sports, Science and Technology of Japan, Grant-in-Aid for Young Scientists (B) from the Japan Society for the Promotion of Science, the Translational Research Program, Strategic Promotion for Practical Application of Innovative Medical Technology from AMED; grants from the Uehara Memorial Foundation, Takeda Science Foundation, and the Sumitomo Foundation; and by grants of the German Research Foundation (SFB TRR 57, SFB TRR 219, BO3755/3-1, and BO3755/6-1) and the German Ministry of Education and Research (STOP-FSGS-01GM1518A). This work was partly supported by World Premier International Research Center Initiative, Ministry of Education, Culture, Sports, Science and Technology (MEXT), Japan, and by AMED-CREST19gm1210009 to MY.

SUPPLEMENTARY MATERIAL

Supplementary File (PDF)

Supplementary Methods.

Figure S1. Histologic findings in human pyelonephritic kidneys. Histologic analysis of human pyelonephritic kidneys. Periodic acid–Schiff (PAS) staining showed patchy tubulointerstitial scarring in (**A**) geographic pattern, (**B**) intratubular aggregates of neutrophils, and (**C**) multiple PAS-positive casts. Bars = (**A**) 300 μm, (**B**) 50 μm, and (**C**) 200 μm.

Figure S2. Human pyelonephritic kidneys exhibited multiple mononuclear cell aggregates. Histologic analysis of human pyelonephritic kidneys. Periodic acid–Schiff (PAS) staining showed (**A**) a chain of aggregates in the subcapsular area and cortico-medullary area and (**B**) an aggregate within the renal capsule, (**C**) the hilus area, and (**D**) submucosal area in the urinary tract. Yellow boxes indicate the localization of inflammatory cell aggregates. Bars = (**A**) 300 μm and (**B–D**) 200 μm.

Figure S3. α-Smooth muscle actin (α-SMA)-positive blood vessels and podoplanin-positive lymphatic vessels are detectable around tertiary lymphoid tissues in the pyelonephritic kidneys. Histologic analysis of human pyelonephritic kidneys. (**A,C**) Periodic acid–Schiff (PAS) staining showed inflammatory cell aggregates. (**B,D**) Immunofluorescence of podoplanin (lymphatic vessel marker) and α-SMA showed that α-SMA-positive arteries and lymphatic vessels were detectable around inflammatory cell aggregates. Parts (**A,B**) and (**C,D**) are serial sections. The white dotted line in (**B,D**) indicates inflammatory cell aggregates. Bars = 50 μm.

Figure S4. Tertiary lymphoid tissues (TLTs) in aged human kidneys were detected in subcapsular, perivascular, and periglomerular areas. Histologic analysis of aged human kidneys. Periodic acid–Schiff (PAS) staining of (**A**) subcapsular, (**B**) perivascular, and (**C**) periglomerular areas. (**D–F**) Immunofluorescence of CD3ε (a T-cell marker) and CD20 (B-cell marker). The white dotted line in parts (**D**), (**E**), and (**F**) indicate localization of the renal capsule, artery, and glomerulus, respectively. Bars = (**A–C**) 200 μm and (**D–F**) 50 μm.

Figure S5. Larger aggregates were detected in more highly injured areas in pyelonephritic kidneys. Histologic analysis of human pyelonephritic kidneys. Periodic acid–Schiff (PAS) staining of the renal cortex with (**A**) mildly, (**B**) moderately, and (**C**) highly injured areas. (**D**) Masson trichrome (MTC) staining of the renal medulla with a highly injured area. The yellow boxes in parts (**B,C**) show the localization of TLT. Bars = (**A–D**) 200 μm.

Figure S6. Foxp3-positive cells were detected within TLTs in human kidneys. Immunohistochemical analysis of human pyelonephritic kidneys. Immunohistochemical analysis of Foxp3 in human TLTs showed the presence of Foxp3-positive cells within TLTs. The yellow box in part (**A**) is magnified in part (**B**). Bars = 20 μm.

Figure S7. Germinal center was composed of 2 subdomains, a light zone and a dark zone. Immunohistochemical analysis of germinal centers in human pyelonephritic kidneys. (**A**) Immunohistochemical analysis of CD21 and (**B**) immunofluorescence of CD21 and Ki67 in human TLTs showed that germinal centers in TLTs were composed of 2 compartments. One is characterized by CD21–strongly positive follicular dendritic cells (FDCs) with scattered cell proliferation, and the other is characterized by CD21–weakly positive FDCs with proliferating cell cluster, which seem to correspond to light zone and dark zone in secondary lymphoid organs, respectively. Bars = 50 μm.

Figure S8. $Foxp3^+$ regulatory T cells were detectable within mouse TLTs and the numbers were decreased by Dex treatment. (**A**) Immunofluorescence of CD3ε and Foxp3 in mouse TLTs 45 days after IRI with or without treatment of Dex (Figure 6a). (**B**) *CD4* and *Foxp3* mRNA levels in the IRI kidneys (35: aged kidneys 35 days after 45-minute IRI; 45: aged kidneys 45 days after 45-minute IRI; 45 Dex: aged kidneys 45 days after 45-minute IRI treated with Dex from day 35 to 45). Bars = (**A**, left) 50 μm and (**A**, right) 10 μm. Arrowheads indicate CD3ε and Foxp3–double positive cells. In part (**B**), values are means ± SD. Statistical significance was assessed using 1-way ANOVA with Bonferroni. $^*P < 0.01$.

Figure S9. The number and stage of renal TLTs were comparable between aged patients with or without a reduced GFR and proteinuria. Quantification of TLT numbers and TLT stages of aged patients with or without a reduced GFR (eGFR < 60 ml/min per 1.73 m^2) as well as those with or without proteinuria among aged patients with renal TLTs. Number of (**A,D**) total TLTs and (**B,E**) advanced-stage TLT per section and (**C,F**) relative frequencies of stage I, II, and III TLTs in the kidneys of aged patients with or without a reduced GFR (eGFR < 60 ml/min per 1.73 m^2) ($n = 13$ and $n = 20$, respectively), and aged patients with or without proteinuria ($n = 8$ and $n = 25$,

respectively). (**A,B,D,E**) Values are means ± SD. (**C,F**) The difference in proportion of advance-stage CKD (stage II and III TLTs) was analyzed. The numbers of TLTs were shown as the numbers per unit area of cortex (per mm^2). Statistical significance was assessed using (**A,B,D,E**) a 2-tailed Student's *t* test and (**C,F**) generalized estimating equations. $^*P < 0.01$. Proteinuria positive was defined as more than 1+ in urine dipstick test.

Table S1. Markers related with TLTs in human kidneys.

Table S2. The quantitative difference in TLT numbers and percentages of advanced TLTs in Figure 5.

Table S3. The quantitative difference in TLT numbers and percentages of advanced TLTs in Figure 6.

Table S4. The quantitative difference in TLT numbers and percentages of advanced TLTs in aged and pyelonephritic human kidneys in Figure 8.

Table S5. Primer sequences used for real-time PCR.

REFERENCES

1. Sato Y, Yanagita M. Immunology of aging kidney. *Nat Rev Nephrol*. 2019;15:625–640.
2. Pitzalis C, Jones GW, Bombardieri M, Jones SA. Ectopic lymphoid-like structures in infection, cancer and autoimmunity. *Nat Rev Immunol*. 2014;14:447–462.
3. Neyt K, Perros F, GeurtsvanKessel CH, Hammad H, Lambrecht BN. Tertiary lymphoid organs in infection and autoimmunity. *Trends Immunol*. 2012;33:297–305.
4. Ansel KM, Ngo VN, Hyman PL, et al. A chemokine-driven positive feedback loop organizes lymphoid follicles. *Nature*. 2000;406:309–314.
5. van de Pavert SA, Oliver BJ, Goverse G, et al. Chemokine CXCL13 is essential for lymph node initiation and is induced by retinoic acid and neuronal stimulation. *Nat Immunol*. 2009;10:1193–1199.
6. Nielen MM, van der Horst AR, van Schaardenburg D, et al. Antibodies to citrullinated human fibrinogen (ACF) have diagnostic and prognostic value in early arthritis. *Ann Rheum Dis*. 2005;64:1199–1204.
7. Avouac J, Gossec L, Dougados M. Diagnostic and predictive value of anti-cyclic citrullinated protein antibodies in rheumatoid arthritis: a systematic literature review. *Ann Rheum Dis*. 2006;65:845–851.
8. Humby F, Bombardieri M, Manzo A, et al. Ectopic lymphoid structures support ongoing production of class-switched autoantibodies in rheumatoid synovium. *PLoS Med*. 2009;6:e1.
9. Ge C, Tong D, Liang B, et al. Anti-citrullinated protein antibodies cause arthritis by cross-reactivity to joint cartilage. *JCI Insight*. 2017;2:93688.
10. Sato Y, Mii A, Hamazaki Y, et al. Heterogeneous fibroblasts underlie age-dependent tertiary lymphoid tissues in the kidney. *JCI Insight*. 2016;1:e87680.
11. Sato Y, Yanagita M. Resident fibroblasts in the kidney: a major driver of fibrosis and inflammation. *Inflamm Regen*. 2017;37:17.
12. Steinmetz OM, Velden J, Kneissler U, et al. Analysis and classification of B-cell infiltrates in lupus and ANCA-associated nephritis. *Kidney Int*. 2008;74:448–457.
13. Thaunat O, Field AC, Dai J, et al. Lymphoid neogenesis in chronic rejection: evidence for a local humoral alloimmune response. *Proc Natl Acad Sci U S A*. 2005;102:14723–14728.
14. Hsiao HM, Li W, Gelman AE, Krupnick AS, Kreisel D. The role of lymphoid neogenesis in allografts. *Am J Transplant*. 2016;16:1079–1085.
15. Pei G, Zeng R, Han M, et al. Renal interstitial infiltration and tertiary lymphoid organ neogenesis in IgA nephropathy. *Clin J Am Soc Nephrol*. 2014;9:255–264.
16. Segerer S, Schlondorff D. B cells and tertiary lymphoid organs in renal inflammation. *Kidney Int*. 2008;73:533–537.
17. Srivastava A, Palsson R, Kaze AD, et al. The prognostic value of histopathologic lesions in native kidney biopsy specimens: results from the Boston Kidney Biopsy Cohort Study. *J Am Soc Nephrol*. 2018;29:2213–2224.
18. Fogo AB, Lusco MA, Najafian B, Alpers CE. AJKD Atlas of Renal Pathology: chronic pyelonephritis. *Am J Kidney Dis*. 2016;68:e23–e25.
19. Fogo AB, Lusco MA, Najafian B, Alpers CE. AJKD Atlas of Renal Pathology: acute pyelonephritis. *Am J Kidney Dis*. 2016;68:e21–e22.
20. Heesters BA, Myers RC, Carroll MC. Follicular dendritic cells: dynamic antigen libraries. *Nat Rev Immunol*. 2014;14:495–504.
21. Miyara M, Yoshioka Y, Kitoh A, et al. Functional delineation and differentiation dynamics of human CD4+ T cells expressing the FoxP3 transcription factor. *Immunity*. 2009;30:899–911.
22. Hori S, Nomura T, Sakaguchi S. Control of regulatory T cell development by the transcription factor Foxp3. *Science*. 2003;299:1057–1061.
23. Mesin L, Ersching J, Victora GD. Germinal center B cell dynamics. *Immunity*. 2016;45:471–482.
24. Krautler NJ, Kana V, Kranich J, et al. Follicular dendritic cells emerge from ubiquitous perivascular precursors. *Cell*. 2012;150:194–206.
25. Sato E, Olson SH, Ahn J, et al. Intraepithelial CD8+ tumor-infiltrating lymphocytes and a high CD8+/regulatory T cell ratio are associated with favorable prognosis in ovarian cancer. *Proc Natl Acad Sci U S A*. 2005;102:18538–18543.
26. Thaunat O, Patey N, Caligiuri G, et al. Chronic rejection triggers the development of an aggressive intragraft immune response through recapitulation of lymphoid organogenesis. *J Immunol*. 2010;185:717–728.
27. Chang A, Henderson SG, Brandt D, et al. In situ B cell-mediated immune responses and tubulointerstitial inflammation in human lupus nephritis. *J Immunol*. 2011;186:1849–1860.
28. Sato Y, Yanagita M. Functional heterogeneity of resident fibroblasts in the kidney. *Proc Jpn Acad Ser B Phys Biol Sci*. 2019;95:468–478.
29. Sato Y, Yanagita M. Immune cells and inflammation in AKI to CKD progression. *Am J Physiol Renal Physiol*. 2018;315:F1501–F1512.
30. Lehmann-Horn K, Wang SZ, Sagan SA, et al. B cell repertoire expansion occurs in meningeal ectopic lymphoid tissue. *JCI Insight*. 2016;1:e87234.
31. Fletcher AL, Acton SE, Knoblich K. Lymph node fibroblastic reticular cells in health and disease. *Nat Rev Immunol*. 2015;15:350–361.
32. Hu D, Mohanta SK, Yin C, et al. Artery tertiary lymphoid organs control aorta immunity and protect against atherosclerosis via vascular smooth muscle cell lymphotoxin beta receptors. *Immunity*. 2015;42:1100–1115.
33. Delventhal S, Hensel A, Petzoldt K, Pabst R. Effects of microbial stimulation on the number, size and activity of bronchus-associated lymphoid tissue (BALT) structures in the pig. *Int J Exp Pathol*. 1992;73:351–357.
34. Hwang JY, Randall TD, Silva-Sanchez A. Inducible bronchus-associated lymphoid tissue: taming inflammation in the lung. *Front Immunol*. 2016;7:258.
35. Katakai T. Marginal reticular cells: a stromal subset directly descended from the lymphoid tissue organizer. *Front Immunol*. 2012;3:200.
36. Furman D, Chang J, Lartigue L, et al. Expression of specific inflammasome gene modules stratifies older individuals into two extreme clinical and immunological states. *Nat Med*. 2017;23:174–184.